

RESEARCH

Open Access



Functions of aldolase in lipid synthesis of *Schizochytrium* sp. by gene disruption to switch carbon metabolism

Yiting Zhang^{1,2}, Xuejun Wu¹, Xiaoyun Guo³, Keyan Li¹, Yinghua Lu^{1,2}, Xihuang Lin⁴ and Xueping Ling^{1,2*}

Abstract

Background As a key rate-limiting enzyme in the glycolytic pathway of cells, aldolase affects the distribution of intracellular carbon flux and determines the overall ability of subsequent cell metabolism, which are mainly reported in the medical related researches, but rarely involved microorganisms. In this study, the aldolase gene of *Schizochytrium limacinum* SR21 (*ALDOA*) was knocked out to explore the effect of regulating carbon flux on cell growth and lipid synthesis.

Results The knockout of *ALDOA* showed an adverse effect on cell growth and total lipids production, which was decreased by 9.6% and 23.2%, respectively, but helped to improve the synthetic ability of polyunsaturated fatty acids (PUFAs), in which the proportion of docosahexaenoic acid (DHA) increased by 22.9%. Analysis of phospholipomics, real-time quantitative PCR and metabolomics revealed that the knockout of *ALDOA* weakened the glycolysis pathway and tricarboxylic acid cycle to inhibit cell growth, and lowered the Kennedy pathway to reduce the production of total lipids and the synthesis of phospholipids to affect cell metabolism. Correspondingly, the knockout of *ALDOA* enhanced the metabolic flux of the pentose phosphate pathway to provide more reducing power for PUFAs accumulation and improved the glycerophosphorylcholine acylation pathway to promote the accumulation of DHA.

Conclusions *ALDOA* knockout redistributes the carbon metabolic flux in cells, by weakening the glycolysis, tricarboxylic acid cycle and glyceride synthesis pathway to inhibit cell growth and total lipid production, and strengthening the pentose phosphate pathway and glycerophosphorylcholine acylation pathway to increase the synthesis of PUFAs and DHA accumulation. This study provides a new idea for identifying the aldolase function in microorganisms and a metabolic strategy to improve DHA accumulation in *Schizochytrium*.

Keywords *Schizochytrium*, DHA, Aldolase, Carbon metabolism, Phospholipids

*Correspondence:

Xueping Ling
xpling@xmu.edu.cn

¹ Department of Chemical and Biochemical Engineering, College of Chemistry and Chemical Engineering, Xiamen University, Xiamen, People's Republic of China

² Xiamen Key Laboratory of Synthetic Biotechnology, Xiamen University, Xiamen, People's Republic of China

³ College of Chemical Engineering and Materials Science, Quanzhou Normal University, Quanzhou, People's Republic of China

⁴ Analysis and Test Center, Ministry of Natural Resources, Third Institute of Oceanography, Xiamen 361005, People's Republic of China

Introduction

As a kind of oleaginous fungi, *Schizochytrium limacinum* owns the oil content of 50~70% of cell dry weight, and a fast growth rate [1]. In recent years, *Schizochytrium* has been highly concerned by academic and industrial researchers due to it can produce a large number of functional substances with commercial value, such as squalene, carotenoids and polyunsaturated fatty acids (PUFAs). In particular, it can synthesize docosahexaenoic acid (DHA) and eicosapentaenoic acid (EPA),



© The Author(s) 2024. **Open Access** This article is licensed under a Creative Commons Attribution-NonCommercial-NoDerivatives 4.0 International License, which permits any non-commercial use, sharing, distribution and reproduction in any medium or format, as long as you give appropriate credit to the original author(s) and the source, provide a link to the Creative Commons licence, and indicate if you modified the licensed material. You do not have permission under this licence to share adapted material derived from this article or parts of it. The images or other third party material in this article are included in the article's Creative Commons licence, unless indicated otherwise in a credit line to the material. If material is not included in the article's Creative Commons licence and your intended use is not permitted by statutory regulation or exceeds the permitted use, you will need to obtain permission directly from the copyright holder. To view a copy of this licence, visit <http://creativecommons.org/licenses/by-nc-nd/4.0/>.

and has become the main source of DHA in industrial production.

At present, the existing related researches of *Schizochytrium* mainly focus on the regulation of fatty acid and the glyceride synthesis pathways, and few reports to study the effect of mediating carbon metabolism on its lipid synthesis. Chang found more carbon skeleton acetyl coenzyme A (acetyl CoA) and reduced nicotinamide adenine dinucleotide phosphate (NADPH) were rerouted to the fatty acid synthesis pathway to promote the synthesis of PUFAs in *Mortierella alpina* by knocking down the encoded heterologous trimer adenosine monophosphate-activated protein kinase subunit (MaSnf4) [2]. Bhutada eliminated intracellular glycogen accumulation by knocking out the glycogen synthase gene in *Yarrowia lipolytica*, which increased the accumulation of triglyceride (TAG) by 52% without affecting cell proliferation [3]. It suggests the regulation of carbon flux is also an important strategy to affect the synthesis and distribution of lipids.

Fructose-1, 6-bisphosphate aldolase (FBA, referred to as 'aldolase') is a ubiquitous cytoplasmic enzyme that catalyzes the fourth step of glycolysis, making the cleavage of fructose-1, 6-bisphosphate into two trisaccharide phosphates: glyceraldehyde-3-phosphate (GAP) and dihydroxyacetone phosphate (DHAP) [4]. Aldolase not only plays a central role in glycolysis, but also plays an important role in gluconeogenesis and fructose metabolism [5], affecting the overall carbon flux of cells and further change cell metabolism. Li found that the deletion of aldolase in tumor cells of mouse released the inhibition on glucose-6-phosphate dehydrogenase (G6PDH), resulting in an increase in the flow of pentose phosphate pathway (PPP) to meet the needs of bioenergy and biosynthesis in the progression of hepatoma cells [6]. The change of this new metabolic pathway enables cancer cells to provide NADPH by up-regulating PPP. It means the flux of PPP can be mediated by regulating the glycolytic pathway. When the glycolysis is inhibited, the flow of glucose to the PPP increases [7], thereby promoting the increase of NADPH, which is the reducing power for fatty acids synthesis [8]. Shino carried out nitrosation stress in *Saccharomyces cerevisiae*, and the activity of aldolase was inhibited, which led to the transformation of glycolysis pathway to PPP, thereby increasing the intracellular NADPH content and enhancing the tolerance of yeast to nitrosation stress [9]. When NADPH content is high, the proportion of unsaturated fatty acids usually increases [10].

The current research of aldolase mainly involves animal cells, cancer diseases and other related fields, and there are few studies on the algae and microorganisms. Therefore, the function of aldolase gene (*ALDOA*) on cell growth and lipid synthesis in *Schizochytrium limacinum*

SR21 (*S. limacinum* SR21) was explored in this study. Phospholipidomics and metabolomics techniques were used to analyze and reveal the regulatory mechanism of aldolase on the carbon flux of *Schizochytrium* and lipid synthesis. It enriches the functional study of aldolase and provides new ideas for the regulation of lipid synthesis in *Schizochytrium*.

Results and discussion

Construction of *ALDOA* knockout strain

As shown in Fig. 1a, upstream and downstream sequences were successfully amplified using the retrieved *ALDOA* sequence (PF00274) as a template. Figure 1b showed the pBlue-zeo-*ALDOA* knockout plasmid was also successfully constructed, which was electroporated into the wild-type competent cells of *Schizochytrium* using homologous recombination. The positive transformants were screened by 50 mg/L bleomycin resistance plate (Fig. S1a). After genome extraction and PCR amplification, the homologous arm fragment was sequenced. The results showed that this fragment was the imported target fragment (Fig. S1b), indicating that *ALDOA* had been successfully replaced by the bleomycin gene in *S. limacinum* SR21, and an *ALDOA* knockout (Δ *ALDOA*) strain was obtained.

Effects of *ALDOA* knockout on cell growth and lipid synthesis

Figure 2a presented that the knockout of *ALDOA* had a remarkable inhibitory effect on the cell growth and total lipids production of *S. limacinum* SR21. Compared with the wild type, the former was reduced by up to 40.61% at 96 h, and the latter was decreased by up to 49.34% at 72 h. The wild-type strain entered a stable period at 120 h, which also reached the maximum lipid production. The dry cell weight (biomass) and lipid yield of the Δ *ALDOA* strain were lower than those of the wild-type strain during the whole fermentation process, which reached the highest biomass and lipid yield at 168 h, which were lowered by 9.6% and 23.2% than the highest values of the wild-type strain ($p < 0.05$), respectively. Figure 2b showed that although the Δ *ALDOA* strain used more glucose in the early stage than the wild-type strain, the middle and later utilization efficiency was greatly reduced. The wild-type strain basically consumed all the glucose at 120 h, while the Δ *ALDOA* strain only utilized about 50% of the glucose at this time, which was exhausted till 168 h. Figure 2c displayed that the proportion of lipids in biomass in Δ *ALDOA* strain was slightly lower than that in the wild-type strain during the whole growth process (<7.7%), and Fig. 2d exhibited that the non-lipid biomass of Δ *ALDOA* strain was lower than that of the wild-type strain in the early stage, but higher

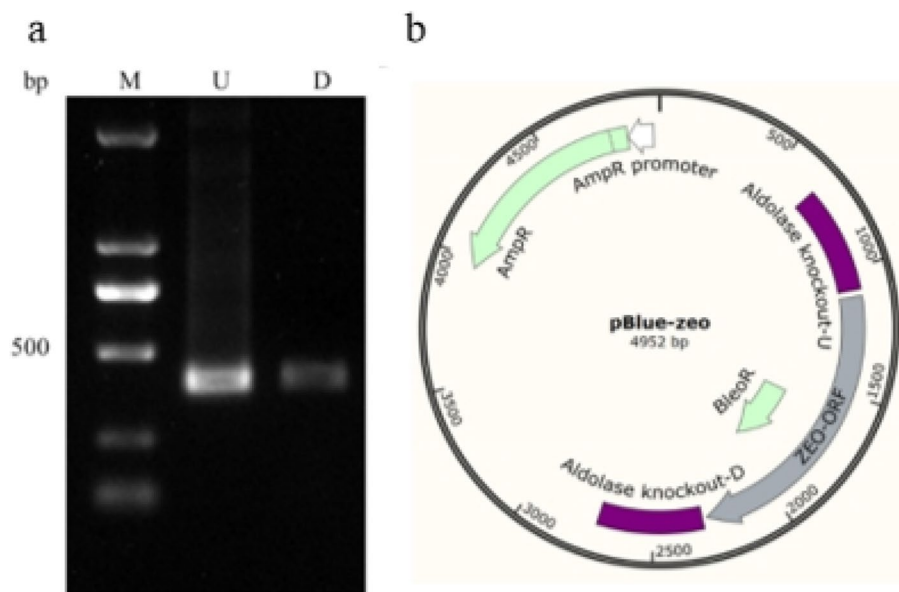


Fig. 1 a PCR amplification of *ALDOA* homologous arms; (b) the structure of pBlue-zeo-*ALDOA*. M: Marker, U: Upstream sequence, D: Downstream sequence

than that of the wild-type strain in the later stage. It's observed that although the knockout of *ALDOA* made the cell grow slowly, the final cell growth could reach the level of the wild-type strain, suggesting that the decrease of biomass and total lipids in Δ *ALDOA* strain is mainly because of the reduced glucose utilization rate, which has little effect on the lipid synthesis capacity of per unit cell.

Effect of *ALDOA* knockout on fatty acids composition

As for the fatty acid composition analysis, the two time points of 72 h and 120 h were selected. It's because the cells were in the middle of logarithmic growth at 72 h to synthesize lipids, and entered the stabel stage to make different types of lipids transformed each other after 120 h, so the analysis of 72 and 120 h can roughly judge the overall growth and metabolism of the cells. As listed in Table 1, the knockout of *ALDOA* obviously reduced the proportion of saturated fatty acids (SFAs), which was about 17.4% lower than that of wild-type strain at 120 h ($p < 0.05$), mainly reflected in the reduction of C16:0 and C14:0; correspondingly, the proportion of PUFAs mainly including DHA, DPA and EPA was drastically increased, which was 28.0% higher than that of the wild-type strain at 120 h ($p < 0.05$), of which the most important DHA presented the increase of about 22.9% ($p < 0.05$), and EPA was also increased by 75.0% ($p < 0.05$). These results indicate that the knockout of *ALDOA* has a great influence on the fatty acids synthesis pathway in *S. limacinum* SR21, which possibly weakens the SFAs synthesis and promotes the PUFAs synthesis accordingly. The catalytic

reaction of aldolase is an important step in the glycolytic pathway, the knockout of which will limit the glycolysis and then affect a series of metabolic pathways such as PPP and fatty acids synthesis.

The fatty acids composition in TAG and phospholipids (PLs) were further analyzed. As summarized in Table 2, for both strains, PUFAs are mainly bound to TAG, the proportion of which in TAG is approximately 35–48%, including DHA, DPA, and EPA; whereas PUFAs in PLs only accounts for 10–15%, mainly consisting of DHA and DPA. It is noteworthy, EPA was not detected in the PLs, indicating that EPA is possibly only bound to TAG, which provides a new idea to study the mechanism of EPA synthesis in *S. limacinum* SR21. In addition, for TAG in two strains, its PUFAs content showed a slight increase at 120 h compared to that at 72 h; for PLs in two strains, its PUFAs content showed the opposite change to that of TAG, in which DHA content at 120 h decreased by 39.7% in wild-type strain and by 25.8% in Δ *ALDOA* strain compared to that at 72 h, respectively. It may be due to PUFAs, especially DHA, is more inclined to bind to PLs first, then migrate from PLs to TAG in the later stage of fermentation for storage [11–13], resulting in the decrease of DHA content in PLs at 120 h. It has been reported that the level of PLs in *Schizochytrium* is closely related to the DHA content in cells [14, 15], and DHA mostly exists in the form of binding to PLs in the early stage, and then transferred to TAG for storage [11, 12].

When comparing the fatty acids composition in two strains, it's found the knockout of *ALDOA* remarkably

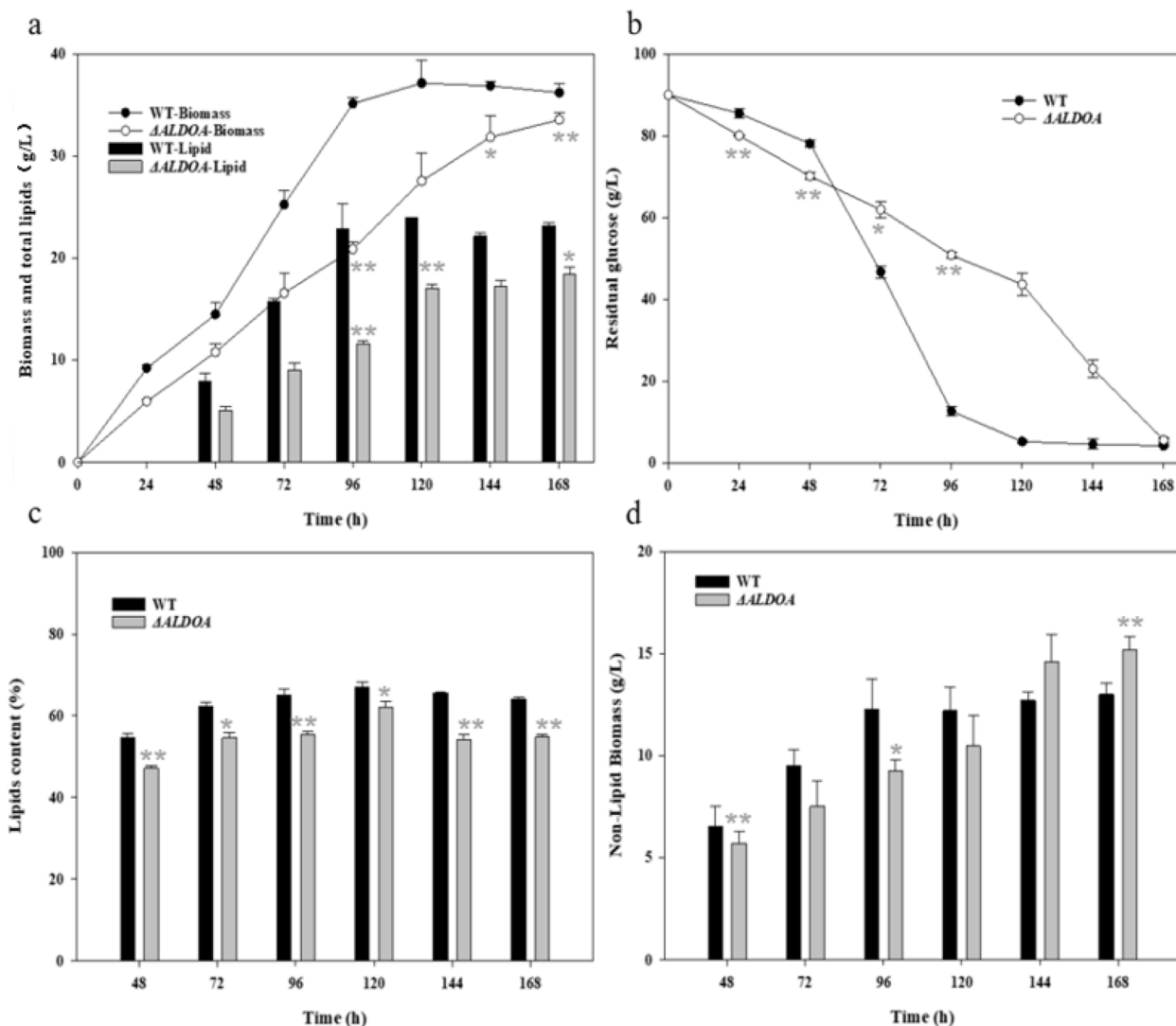


Fig. 2 a Biomass and total lipids, (b) glucose concentration, (c) Lipids content and (d) the non-lipid biomass in the wild-type and $\Delta ALDOA$ strains

Table 1 Fatty acids composition of wild-type and $\Delta ALDOA$ strains

| Fatty acids | 72 h | | 120 h | |
|-------------|-----------|----------------|-----------|----------------|
| | WT | $\Delta ALDOA$ | WT | $\Delta ALDOA$ |
| C14:0 | 2.60±0.05 | 1.22±0.05 | 2.93±0.13 | 1.08±0.07 |
| C15:0 | 1.22±0.30 | 1.50±0.21 | 1.30±0.02 | 1.57±0.19 |
| C16:0 | 49.0±0.47 | 42.1±0.68 | 50.3±0.91 | 40.1±1.65 |
| C17:0 | 0.54±0.16 | 0.62±0.16 | 0.63±0.10 | 0.75±0.23 |
| C18:0 | 1.67±0.02 | 1.88±0.01 | 1.52±0.04 | 1.98±0.14 |
| EPA | 0.26±0.01 | 0.39±0.00 | 0.36±0.02 | 0.63±0.08 |
| DPA | 6.77±0.20 | 8.39±0.08 | 6.73±0.14 | 10.2±0.15 |
| DHA | 34.7±0.72 | 37.1±0.29 | 34.0±0.85 | 41.8±1.17 |
| SFAs | 55.1±1.00 | 47.3±1.11 | 55.1±1.16 | 45.5±2.28 |
| PUFAs | 41.8±0.93 | 45.9±0.37 | 41.1±1.01 | 52.6±1.40 |

enhanced the proportion of PUFAs in TAG, of which the DHA increased by 27.4% and 20.8% at 72 and 120 h, respectively ($p < 0.05$); and reduced the content of SFAs in TAG accordingly, of which the main C16:0 decreased by 46.5% and 36.0% at 72 and 120 h, respectively ($p < 0.01$). For PLs, its DHA proportion in the knockout strain was 15.9% lower than that of the wild-type strain at 72 h, while was almost the same as that of the wild-type strain at 144 h. The above results indicate that *ALDOA* mainly promotes the accumulation of PUFAs in TAG. In view of the reported DHA migration mechanism [11, 12], it's inferred that the knockout of *ALDOA* contributes to the faster transferring of DHA from PLs to TAG. *ALDOA* may be involved in the

Table 2 Fatty acids composition of wild-type and Δ ALDOA strains

| Culture condition | Lipid class | Percent of fatty acids (%) | | | | | | | |
|----------------------|-------------|----------------------------|-----------|-----------|-----------|-----------|-----------|-----------|-----------|
| | | C14:0 | C16:0 | C18:0 | SFAs | EPA | DPA | DHA | PUFAs |
| WT-72 h | TAG | 0.12±0.02 | 52.0±1.27 | 2.43±0.17 | 54.5±2.48 | 0.14±0.01 | 5.64±0.25 | 28.8±1.34 | 34.6±2.56 |
| | PL | 2.03±0.18 | 34.8±1.14 | 13.7±1.02 | 50.5±1.97 | 0.00±0.00 | 3.18±0.36 | 11.1±0.12 | 14.3±1.11 |
| Δ ALDOA-72 h | TAG | 0.42±0.16 | 27.8±1.23 | 4.37±0.98 | 32.6±1.71 | 0.42±0.07 | 8.46±0.45 | 36.7±2.11 | 45.6±3.01 |
| | PL | 2.50±0.00 | 31.5±2.49 | 16.2±1.74 | 50.2±2.63 | 0.00±0.00 | 2.86±0.77 | 9.33±0.47 | 12.2±0.99 |
| WT-120 h | TAG | 0.30±0.01 | 46.9±3.85 | 2.86±0.48 | 50.1±0.98 | 0.22±0.01 | 6.02±0.28 | 30.7±0.78 | 36.9±1.71 |
| | PL | 1.26±0.84 | 25.7±1.45 | 13.2±0.44 | 40.2±0.74 | 0.00±0.00 | 3.09±0.62 | 6.69±0.39 | 9.78±0.84 |
| Δ ALDOA-120 h | TAG | 0.33±0.01 | 30.0±0.45 | 3.3±0.74 | 33.6±0.56 | 0.57±0.08 | 10.3±0.66 | 37.1±1.96 | 48.0±2.34 |
| | PL | 2.23±0.07 | 22.1±1.85 | 12±0.74 | 36.3±0.89 | 0.00±0.00 | 2.87±0.60 | 6.92±0.72 | 9.79±0.63 |

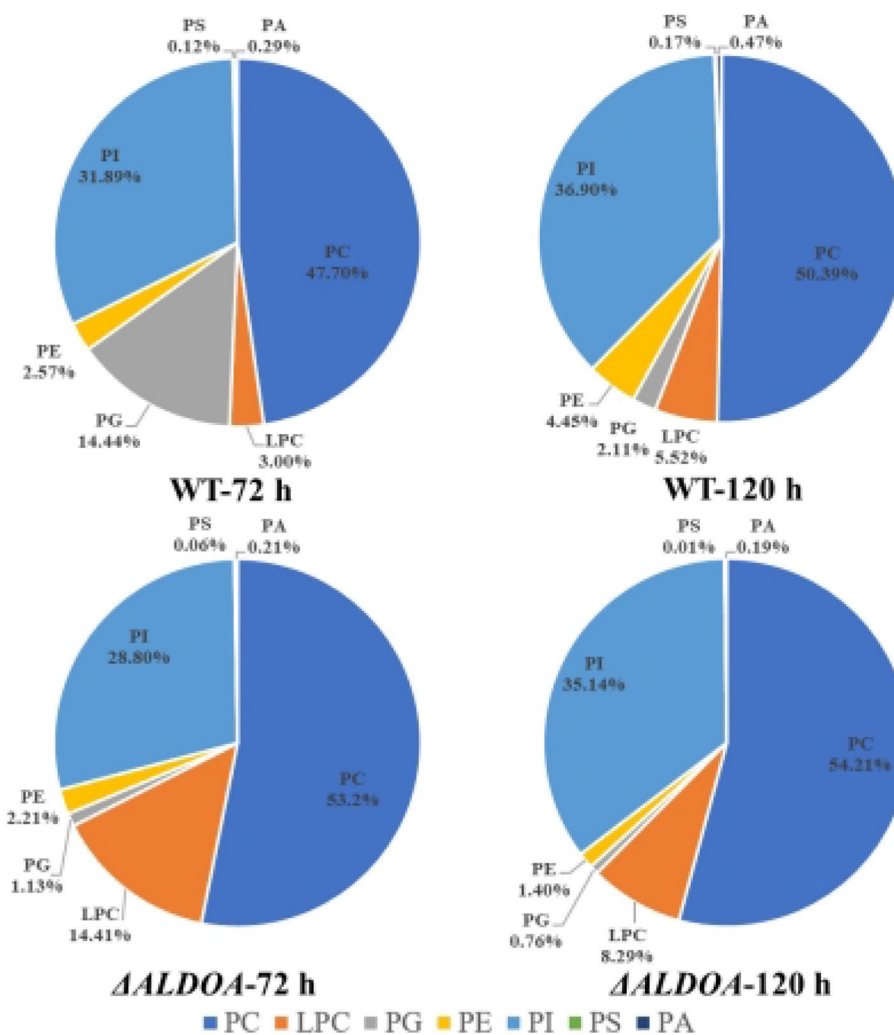


Fig. 3 Percentage of different types of phospholipid at 72 and 120 h in wild-type and Δ ALDOA strains

metabolic regulation of cellular phospholipids, thus affecting the migration and accumulation of DHA.

Effects of *ALDOA* knockout on different phospholipids composition

As plotted in Fig. 3, phosphatidylcholine (PC), phosphatidylinositol (PI) and phosphatidylglycerol (PG) are the main phospholipids in *S. limacinum* SR21, and the most important PC accounts for half of the total phospholipid content. The proportion of PC in *ALDOA* knockout strains increased, which was 11.5% and 7.5% higher than that of wild-type strain at 72 and 120 h, respectively ($p < 0.01$), suggesting that the knockout of *ALDOA* promotes the synthesis of PC. Studies have shown that DHA is initially mainly bound to PC (DHA-PC) and later transferred to TAG [16, 17]. Combining with the increase of DHA content in Δ *ALDOA* strain (Table 1), it is considered that the content of PC is closely related to the synthesis and accumulation of DHA [18, 19]. Lysophosphatidylcholine (LPC) is the main precursor for the synthesis of PC through glycerophosphorylcholine (GPC) acylation pathway [19], which is presumed to be the main pathway to synthesize DHA-PC [20]. The content of LPC in Δ *ALDOA* strain was 4.8 and 1.5 times that of the control group at 72 h and 120 h ($p < 0.05$), respectively, indicating the knockout of *ALDOA* inhibits the conversion of glucose to DHAP, resulting in a decrease of precursor for in PG synthesis and causing slow cell growth of Δ *ALDOA* strain, which is conducive to synthesize LPC and PC to bind more DHA, which is ultimately transferred to TAG for storage.

PG is closely related to cell growth [21], the content of which is usually high in the early and middle stage and low in the later stage of cell growth, due to the sufficient carbon source in the early and middle stages are converted into glycerol 3-phosphate (G3P) from DHAP for the synthesis of PG, and the depleted carbon source in the later period (120 h) lacks of being converted into G3P to synthesize PG. PG content of the knockout strain decreased by 92.2% and 64.0% than that of the wild-type strain at 72 h and 120 h, respectively, indicating the knockout of *ALDOA* inhibits the conversion of glucose to DHAP, resulting in a decrease of precursor for PG synthesis and causing slow cell growth of Δ *ALDOA* strain (Fig. 2a).

PI acts as a signal molecule for cell signal transduction and metabolic regulation [22]. The increase of PI content at 120 h in both strains might be the result of a more active signaling pathway for lipid metabolism and metabolic regulation. A small decrease in PI content in Δ *ALDOA* strain means the signaling pathway for lipid synthesis is slightly hindered (Fig. 2c). What's more, phosphatidylserine (PS) and phosphatidic acid (PA), as

the important components of cell membrane composition [23], also decreased. PG, PI and PS are synthesized via the cytidine diphosphate diacylglycerol (CDP-DAG) pathway using PA as the precursor [24]. All the contents of PG, PI, PS and PA in Δ *ALDOA* strain were reduced compared to the wild-type strain, which demonstrates that *ALDOA* knockout suppresses DHAP synthesis, resulting in the reduction of the precursor flowing to PA and the ultimate decreased synthesis of PG, PI and PS. In addition, PE is considered to be related to the mutual transformation of lipid types in polar lipids, the decrease of which may decline the mobility of cell membrane owing to its head group and anionic properties [13]. PLs are closely related to the function of cell membrane and cell growth. It can be seen that the knockout of *ALDOA* inhibits the synthesis of PA, an intermediate in the Kennedy metabolic pathway, thereby weakening the conversion of PA into other phospholipids. In order to resist the decrease of PG, PI and PS synthesis caused by *ALDOA* knockout, cells strengthen the GPC acylation pathway to synthesize LPC and PC, so as to maintain the function of cell membrane and enable cells to continue to reproduce.

The effect of *ALDOA* knockout on the transcription level of related genes

Acetyl-CoA carboxylase (ACC) is the key initiation enzyme of fatty acids synthesis pathway. The fatty acid synthase gene (*FAS*) encodes a series of proteins related to the synthesis of SFAs via the traditional *FAS* pathway [25]. The chain length factor (*CLF*) gene is located in the anaerobic polyketide synthase (*PKS*) gene cluster and is responsible for chain lengthening during PUFAs synthesis [16]. As plotted in Fig. 4, the transcription level of *ACC* at 60 h was basically the same as that of wild-type strain (Fig. 4a), while *FAS* level was higher than that of wild-type strain and *CLF* level was lower than that of wild-type strain (Fig. 4b and c). With the prolonged fermentation of *S. limacinum* SR21, *ACC* level decreased slightly and *FAS* level reduced obviously, while *CLF* level showed a remarkable increase in the middle and later stages of fermentation. These results indicates that the knockout of *ALDOA* does not attenuate the fatty acid synthesis capacity of per unit cell too much (Fig. 4a and Fig. 2c), but changes the metabolic flow of *FAS* and *PKS* pathways. The decrease of *FAS* pathway (Fig. 4b) suppresses the synthesis of SFAs, and the increase of *PKS* pathway (Fig. 4c) promotes the accumulation of PUFAs. The decrease of total lipids is more due to the inhibition of cell growth in the early stage (Fig. 2a). The accumulation of lipids in *Schizochytrium* was mainly concentrated after 48 h. The glucose consumed before this time point was mainly used for cell growth. In order to resist the negative effects of *ALDOA* knockout on cell growth in the

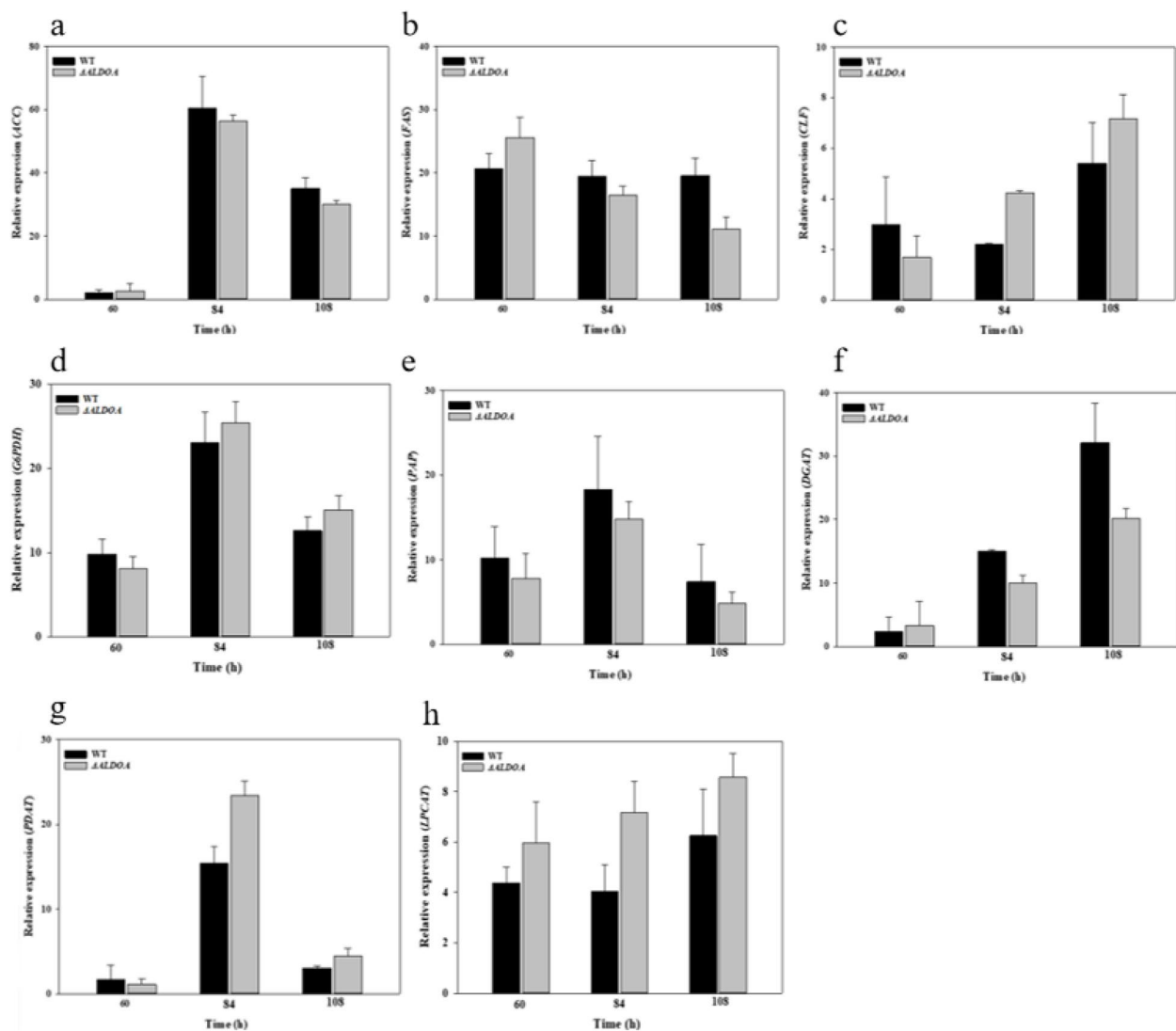


Fig. 4 The transcription level of related genes in the wild-type and Δ ALDOA strains. **a** ACC; **b** FAS; **c** CLF; **d** G6PDH; **e** PAP; **f** DGAT; **g** PDAT; **h** LPCAT

early stage, the mutant strain consumed more glucose to regulate cell performance (Fig. 2b). As shown in Fig. 2c, when the bacteria entered the rapid lipid synthesis period after 48 h later, the lipid content of the Δ ALDOA strain was not much different from that of the wild type, which means that the unit cell lipid synthesis ability of the two strains was almost similar, and the lower glucose consumption after 72 h in the ALDOA knockout strain is due to the inhibited cell growth. G6PDH catalyzes the oxidation of glucose-6-phosphate to 6-phosphogluconolactone, accompanied by the production of NADPH, which is considered to be the metabolic node between glycolysis and PPP [26]. The transcription level of G6PDH in Δ ALDOA strain presented the similar change to CLF

compared with that of wild-type strain (Fig. 4d), falling first and then rising, which indicates that the knockout of ALDOA enhances the metabolic flow of PPP, thus providing more reducing power for cell metabolism, which is conducive to PUFAs synthesis [27, 28].

PA can be converted into diacylglycerol (DAG) by hydrolyzation of phosphatidic acid phosphatase (PAP), and DAG is subsequently catalyzed by diacylglycerol acyltransferase (DGAT) to produce TAG. The decrease of PAP and DGAT transcription levels (Fig. 4e and f) indicates that ALDOA knockout blocks the Kennedy pathway and eventually leads to the decreased glycerides accumulation due to the inhibited synthesis of DHAP. Phospholipid diacylglycerol choline phosphate transferase

(PDAT) catalyzes the transacylation reaction of PC and DAG to produce TAG [29]. Previous studies have elucidated that DHA is first bound to PC after synthesis, and then transferred to TAG for storage by PDAT catalysis [11, 12]. Figure 4g showed that the transcription level of *PDAT* was apparently increased in the Δ *ALDOA* strain, indicating that *ALDOA* knockout promotes the migration of DHA from PC to TAG. Zhang found that the increase of *PDAT* transcription level made more PC converted into glycerides, which may be an important factor leading to the increase of PUFAs proportion [30]. Lysophosphatidylcholine acyltransferase (*LPCAT*) is responsible for the acylation of LPC to PC in the GPC acylation pathway and is believed to mainly catalyze the acylation of PUFAs [31]. The profound improvement of the transcription level of *LPCAT* in the Δ *ALDOA* strain (Fig. 4h) illustrates that the GPC acylation pathway is enhanced to produce PC, which is conducive to the binding of DHA to PC. It is consistent with the increase of the proportion of PC and LPC in PLs content after *ALDOA* knockout observed in Fig. 3. Hence, it is speculated that the knockout of *ALDOA* weakens the synthesis of TAG by the Kennedy pathway and strengthens the PDAT catalytic pathway to synthesize TAG through the PC pathway. Due to PC mainly binds to PUFAs such as DHA, it enhances the transferring process of DHA and eventually facilitates the accumulation of DHA in TAG (Table 2).

Analysis of reactive oxygen species in Δ *ALDOA* strain

PUFAs are easily oxidized by free radicals in cells. The content of reactive oxygen species (ROS) in cells was shown in Fig. 5, and the fluorescence intensity reflected the degree of oxidative damage in cells. After *ALDOA* knockout, the intracellular fluorescence intensity decreased in both time points, indicating a decrease of

ROS content. In addition, the ROS content of the two strains in the early growth stage was lower than that in the late growth stage. The main reason for the change is that in the early stage of fermentation, the metabolic rate of the cell growth is slow, less ROS are produced, and rich nutrients can also play a protective role. Liu found that under nitrogen limitation conditions, oleaginous microalgae can induce oxidative stress and redistribute lipids and fatty acids [32]. The lower oxidative stress environment is conducive to cell metabolism and reduces the oxidation of PUFAs, which increases the proportion of PUFAs in Δ *ALDOA* strain.

Metabolomic analysis of Δ *ALDOA* strain

After comparing the tested results with the NIST 2.2 database, 35 related metabolites were identified, which were normalized by Z-value conversion and the heat map was drawn. Figure 6 showed the difference in metabolism of *S. limacinum* SR21 after *ALDOA* knockout, mainly involving the glycolytic pathway, the tricarboxylic acid (TCA) cycle, the PPP, the fatty acid synthesis pathway, and the synthesis of amino acids, carbohydrates and sterols. According to the position of the identified different metabolites corresponding to the genome encyclopedia (KEGG), some metabolic processes in *S. limacinum* SR21 were mapped in Fig. 7, so as to analyze and discuss the effect of *ALDOA* knockout on cell metabolism.

The glucose content in the *ALDOA* knockout strain showed no clear change at 72 h and a decrease at 120 h. Combining with the remaining glucose in the fermentation process shown in Fig. 2b, it can be seen that the intake and utilization of glucose in Δ *ALDOA* strain is faster than that of wild-type strain in the early growth stage, which makes the other metabolites at this stage exhibit the corresponding increase. It may be due to the

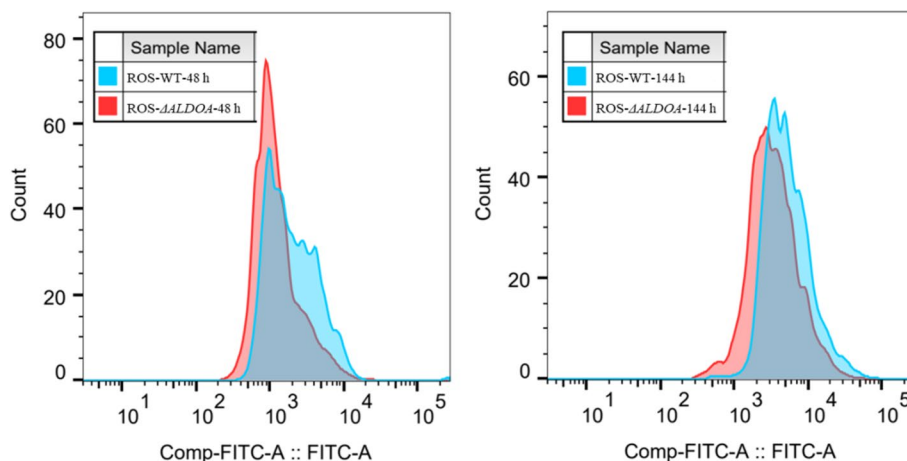


Fig. 5 Intracellular reactive oxygen content of wild-type and Δ *ALDOA* strains at different times

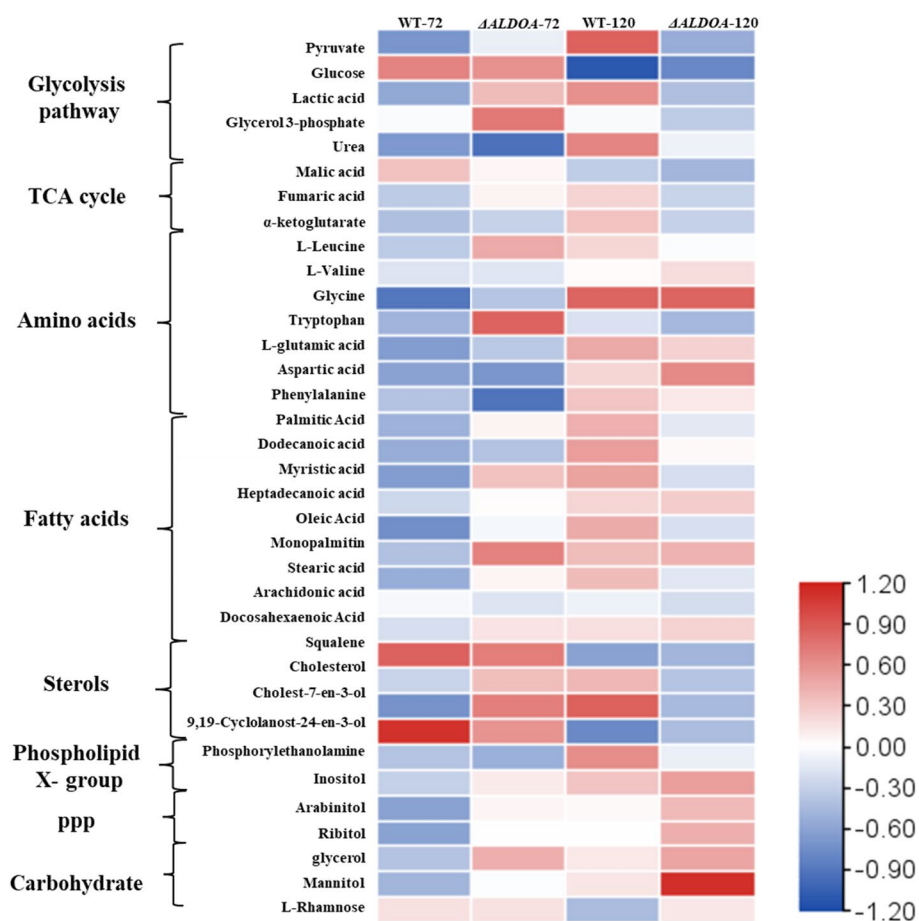


Fig. 6 Clustering analysis of intracellular metabolites between wild-type and Δ ALDOA strains. Note: Red represents a higher level, blue represents a lower level

fact that cells enhance the overall metabolism to resist the effect of ALDOA knockout. With the prolongation of fermentation time, the glycolysis pathway and TCA cycle in the mutant strain decreased, accompanied by the reduced glucose utilization, making the intake and intracellular content of glucose slightly lower than that of the wild-type strain. The content of G3P was also lower than that of the wild-type strain at the late stage of fermentation (120 h), because the knockout of ALDOA directly resulted in a decrease in its precursor, which affects the flux distribution of carbon metabolism in *Schizochytrium*.

Knockout of ALDOA enhanced the content of metabolites in the PPP, of which arabitol and ribitol increased by 4.06 times and 7.84 times at 120 h ($p < 0.05$), respectively, indicating that the enhanced PPP in Δ ALDOA strain could provide more reducing power of NADPH for cell growth and fatty acids synthesis of *Schizochytrium* [27, 28]. In addition, the knockout of ALDOA also promoted the non-oxidative phase of the PPP pathway to provide glyceraldehyde-3-phosphate as a supplementary

carbon flow in the second stage of the glycolysis pathway to produce pyruvate, which can be converted into acetyl-CoA. SFAs presented a decrease and DHA displayed an increase at 120 h in Δ ALDOA strain compared with the wild-type strain. In addition, the inositol content in the knockout strain was 3.00 times higher than that in the wild-type strain ($p < 0.05$) at 120 h. Inositol is a signal molecule against oxidative stress and regulates cell metabolism [33]. Liu found that the lipid and DHA production was greatly increased after exogenous addition of inositol during the culture of *Schizochytrium limacinum* [34]. Mannitol was also 1.23 times higher than that of the wild-type strain ($p < 0.05$). Mannitol can scavenge hydroxyl radicals and protect cells from oxidative stress [35]. Han added mannitol exogenously during the culture of *Schizochytrium limacinum* [36], and found that ROS content decreased, and cell biomass and lipid content increased. What's more, the content of glycine increased, which can provide precursors for the synthesis of glutathione and enhance the antioxidant capacity of cells [23]. It's consistent with the results of Fig. 5.

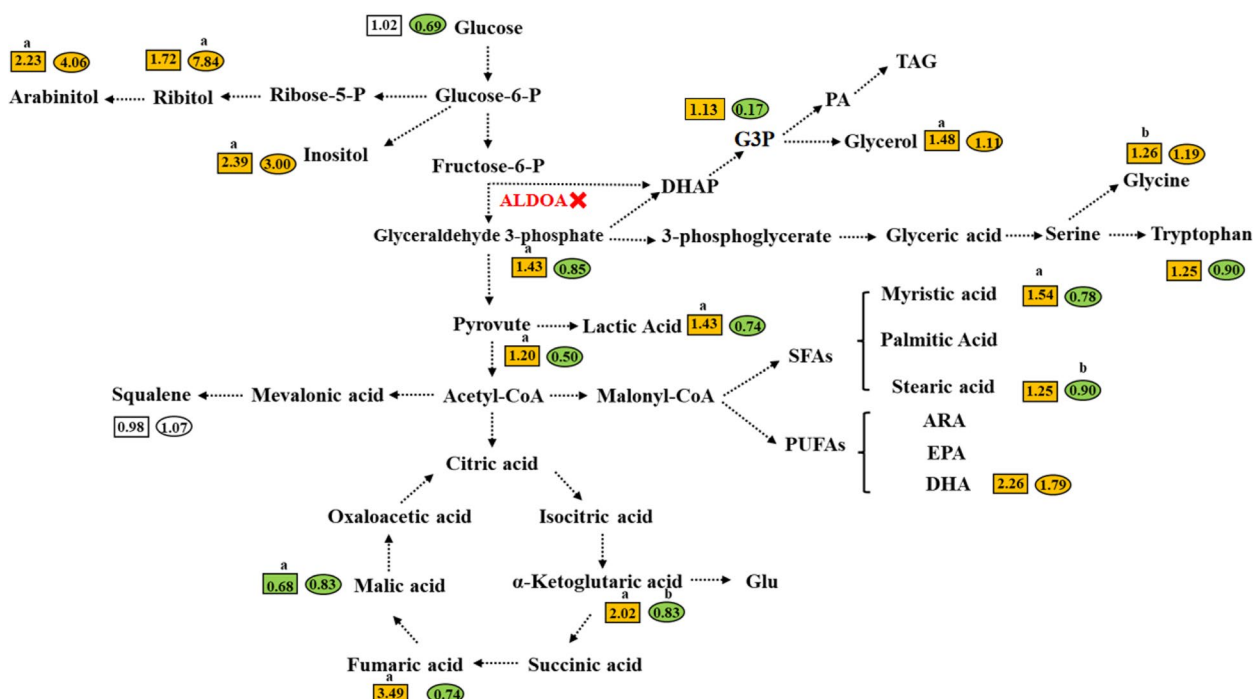


Fig. 7 Changes in intracellular metabolites of $\Delta ALDOA$ strains compared with that of the wild-type at different fermentation stages. Note: Yellow: increase; green: reduction; white: little change; rectangle: 72 h; oval: 120 h; (a) $p < 0.05$ or (b) $p < 0.01$

Proposed metabolic mechanism of *ALDOA* knockout

S. limacinum SR21

After *ALDOA* knockout, the cell growth and total lipid synthesis were significantly lower than those of the wild-type strain (Fig. 2a). As constructed in Fig. 8, the suppressed glycolysis pathway in $\Delta ALDOA$ strain greatly reduces the production of GAP and DHAP, which attenuates the metabolic flow of the Kennedy pathway, thereby reducing TAG synthesis (Fig. 2 and Fig. 4) and weakening the CDP-DAG phospholipid synthesis of PG, PI and PS to inhibit cell growth (Fig. 3 and Fig. 4). Accordingly, *ALDOA* knockout facilitates the carbon flux of the PPP, providing more reducing power for PUFAs synthesis and reducing the production of ROS to inhibit the oxidative decomposition of PUFAs (Fig. 4–6). In addition, the decrease of phospholipids synthesis from the Kennedy pathway induces the synthesis of PC by the GPC acylation pathway (Fig. 3 and 4). PC can not only regulate cell membrane function to maintain cell growth, but also contribute to DHA binding to PC and migration of DHA from PC to TAG by PDAT catalysis. It eventually improves the content of PUFAs and DHA in $\Delta ALDOA$ strain.

Conclusion

In this study, the effect of *ALDOA* knockout on lipid synthesis in *S. limacinum* SR21 was investigated for the first time. The knockout of *ALDOA* has a significant inhibition on cell growth and lipid production, but has a promoting effect on PUFAs synthesis and DHA accumulation. It's concluded that *ALDOA* knockout weakens the glycolysis and TCA cycle to inhibit cell growth, and reduces DHAP synthesis to attenuate the Kennedy pathway of producing total lipids. In turn, *ALDOA* knockout enhances the PPP to provide more reducing power for PUFAs synthesis, and strengthens the PDAT pathway to promote the accumulation of DHA in TAG. These results suggest that *ALDOA* can profoundly affect the distribution of carbon metabolic flux, which has a great influence on lipid synthesis. Future work can adopt CRISPR or RNA interference technology to regulate *ALDOA* in *Schizochytrium* to improve lipid and DHA production without an obvious inhibition on cell growth.

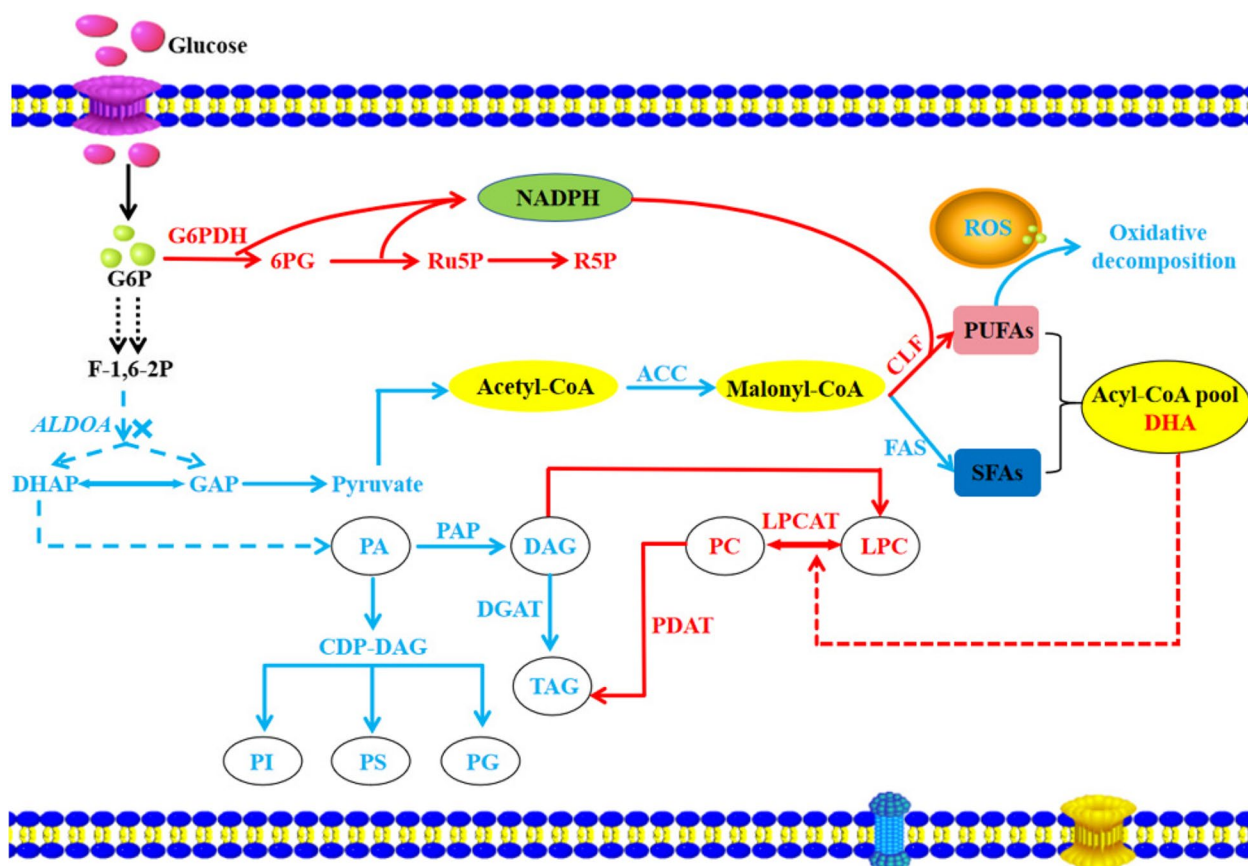


Fig. 8 Effect of *ALDOA* knockout on cell metabolism in *S. limacinum* SR21

Materials and methods

Strains, media, and culture conditions

The *S. limacinum* SR21 was purchased from the American Center for Type Culture Collection (Manassas, VA, USA). The pBlue-zeo vector plasmid was previously constructed and preserved by our laboratory [13].

The seed culture medium contains (g/L): glucose 30, yeast extract 10, CaCl₂ (500×) 2 mL, inorganic salt component A (20×) 50 mL, and pH 6.5. The fermentation medium consists of (g/L) [13]: glucose 90, tryptone 5, corn steep powder 5, inorganic salt component A (20×) 50 mL, CaCl₂ (500×) 2 mL, and pH 6.5. Inorganic salt component A (20×) was the same as that in our previous study [13]. The medium was sterilized at 115 °C for 20 min before use. The trace element and vitamin solutions were filter-sterilized using a 0.2 μm filter.

Activation and culture of *S. limacinum* SR21. The glycerol tube seeds were streaked on solid medium and cultured at 28 °C for 24–48 h to be activated. The single colony was selected and inoculated into the seed medium to be cultured at 28 °C, 200 rpm for 24 h, then transferred to the seed medium for another 24 h, and finally

transferred to 15–20 mL of the fermentation medium in the shake flask for 168 h at 28 °C and 200 rpm.

Construction of *ALDOA* knockout strain

The sequence of aldolase from *Aurantiochytrium limacinum* ATCC MYA-1381 (*S. limacinum* SR21) was searched from the published database (JGI database), and an aldolase gene sequence (PF00274) was found, which belongs to class I aldolase (*ALDOA*). The specific construction of *ALDOA* knockout strain was shown in Fig. S2. The upstream and downstream sequences of 420 bp were amplified, and the restriction sites of Apa I and Xho I were inserted into the upstream primers sequence, and the restriction sites of BamH I and Xba I were inserted into the downstream primers sequence. The upstream and downstream homologous arms were ligated to the bleomycin gene expression cassette of the pBlue-zeo plasmid by enzyme digestion and ligation to obtain the pBlue-zeo-*ALDOA* knockout plasmid. Using this as a template, the DNA fragment containing the upstream homologous arm-bleomycin-downstream homologous arm was amplified by PCR and introduced into the wild-type competent cells of *S. limacinum* SR21

by electroporation. The positive transformants were screened by 50 mg/L bleomycin resistance plate as shown in Fig. S1b.

Measurement of biomass and residual glucose concentration

After shaking well, 1 mL of fermentation broth was centrifuged at 10,000 rpm for 2 min. The cell pellets were washed twice with normal saline, then were vacuum freeze-dried for 24 h to be weighed as the biomass. The supernatant was collected to measure glucose concentration using the 3, 5-dinitrosalicylic acid (DNS) method.

Total lipids extraction and fatty acid composition determination

Five milliliter of fermentation broth was mixed with 5 mL concentrated HCl, which were incubated in a water bath at 65 °C for 45 min to break cell wall. After cooled, 5 mL of *n*-hexane was repeatedly added to extract the lipid until the upper organic phase was colorless. All the extracted organic phases were put together and blown dry by nitrogen, then dried in an oven at 65 °C for 2 h. The sample was weighed as the total lipids.

Total fatty acid production was calculated by subtracting unsaponifiable matter from total lipids. The preparation of fatty acid methyl esters and analysis of fatty acid composition were performed as previously described [13].

Phospholipidomics analysis

Extraction of crude phospholipids from *S. limacinum* SR21 was conducted according to the Bligh-Dyer method [37] with some modification. The detailed steps were as follows: 5 mL of fermentation broth mixed with 2 mL deionized water, 6 mL methanol and 3 mL chloroform were violently vortexed for ultrasonication for 30 min. Three milliliter of deionized water was added and the mixture was violently vortexed for ultrasonication for 30 min. Then, 1 mL of saturated NaCl was added to the solution, which was centrifuged at 4,500×g for 10 min after violent vortex mixing. The lower chloroform layer containing the lipids was transferred to a clean and weighed centrifuge tube, and dried by nitrogen blowing. The obtained sample was stored at -20 °C for use.

Separation of phospholipids was carried out by solid phase extraction (SPE) [13]. The separated phospholipids was analyzed using ultra performance liquid chromatography-mass spectrometry (Waters UPLC Acquity H-Class-Xevo-G2 Q-ToF, Milford, MA, USA). Chromatographic column: ACQUITY UPLC BEH HILIC column (150 mm×2.1 mm×1.7 μm); mobile phase: A is acetonitrile, and B is ammonium formate aqueous solution (20 mM, pH of 3.5 adjusted by 0.1% formic acid); flow

rate: 0.2 mL/min; injection volume: 2 μL; the specific elution procedures was the same as that used in our previous study [13].

Real-time fluorescent quantitative PCR (qRT-PCR)

One milliliter of fermentation broth was centrifuged at 10,000×g for 2 min. The cell pellets were washed twice with normal saline, and quenched with liquid nitrogen, then stored at -80 °C for extracting total RNA using the RNA Plant Plus reagent (TaKaRa, Japan). The extracted RNA (1 μg) was reverse transcribed to cDNA with QuantScript RT Kit reagent (TaKaRa, Japan) according to the manufacturer's instructions. Finally, qRT-PCR amplification was performed using the One Step SYBR PrimeScript PLUS RT-PCR kit (TaKaRa, Japan). Primers used were listed in Table S1.

Determination of reactive oxygen species

The level of reactive oxygen species (ROS) was determined using a cell permeation probe-2', 7'-dichlorodihydrofluorescein diacetate (DCFH-DA) [38]. Loading probe: 1 mL bacterial solution was centrifuged at 10,000×g for 1 min, and the cell pellets were washed twice with phosphate buffer saline (PBS); the appropriate volume of DCFH-DA diluted with PBS at a ratio of 1:1000 was added to completely cover the cells, which were incubated at 37 °C for 20 min; the cells were washed with PBS for 3 times to fully remove DCFH-DA that did not enter the cells, then re-suspended in PBS. Detection: The samples were detected by flow cytometry (FACS Verse flow cytometry, USA) using 488 nm excitation wavelength and 525 nm emission wavelength.

GC-MS metabolomics analysis

The metabolome samples were prepared according to the procedure described by Yu et al. [39]. The obtained samples was determined using Agilent 5977B GC-MS system (Agilent, USA) equipped with an HP-5 capillary column (30 m×0.25 mm, 0.25 μm; Agilent USA). Determination settings: injection volume: 1 μL, injection temperature: 280 °C, split ratio: 1:1; carrier gas: helium (20 cm/s), detector temperature: 280 °C. The column initial temperature was 70 °C, raised to 110 °C at 20 °C/min, then raised to 180 °C at 7 °C/min, then raised to 250 °C at a 5 °C/min, and finally raised to 300 °C at 25 °C/min and maintained for 9 min. The mass scan range was 50–600 m/z. The total tested intracellular metabolites were identified based on the NIST 2.2 database (<https://www.nist.gov/>), and their contents per unit of cells (μg/g DCW) were analyzed using the standard internal method. Finally, the heat map was drawn by TBtools software, and the differential metabolites were analyzed by hierarchical cluster analysis (HCA).

Statistical analysis

In this study, t-test values showed statistical differences between different groups. $0.01 < p < 0.05$ and $p < 0.01$ were considered statistically significant and extremely significant. All experiments were performed in three independent parallel. The values are expressed as mean \pm SD (standard deviation).

Supplementary Information

The online version contains supplementary material available at <https://doi.org/10.1186/s44315-024-00014-6>.

Supplementary Material 1.

Acknowledgements

We gratefully acknowledge the Analysis and Test Center of the Third Institute of Oceanography for its continuous support.

Authors' contributions

XPL and YTZ conceived and designed the research. YTZ and XJW conducted the experiments and wrote the manuscript. YTZ, XYG and KYL analyzed the data. XHL contributed analytical tools. XPL and YHL modified the manuscript. All authors read and approved the manuscript.

Funding

This work was supported by the Natural Science Foundation of Xiamen, China (No.3502Z20227183), the Natural Science Foundation of Fujian Province (2022J05223) and the Quanzhou City Science & Technology Program of China (2021N181S).

Availability of data and materials

The authors can confirm that all relevant data are included in the article and supplementary materials files.

Data availability

No datasets were generated or analysed during the current study.

Declarations

Ethics approval and consent to participate

This study does not contain any studies with human participants or animals performed by any of the authors.

Consent for publication

All authors have seen the manuscript and approved to submit to your journal for publication.

Competing interests

The authors declare no competing interests.

Received: 5 June 2024 Accepted: 29 August 2024

Published online: 01 December 2024

References

- Contreras P, Oviedo C. Potential and future perspectives of *thraustochytrids* in bioremediation. *International Journal of Environmental Science and Technology*. 2023;20:4483–98.
- Chang L, Tang X, Zhang H, Chen YQ, Chen H, Chen W. Improved Lipogenesis in *Mortierella alpina* by Abolishing the Snf4-Mediated Energy-Saving Mode under Low Glucose. *J Agric Food Chem*. 2020Sep 30;68(39):10787–98.
- Bhutada, G.; Kavscek, M.; Ledesma-Amaro, R. Sugar versus fat: elimination of glycogen storage improves lipid accumulation in *Yarrowia lipolytica*. *FEMS Yeast Res*. 2017;17(3):fox020.
- Droppelmann CA, Sáez DE, Asenjo JL, et al. A new level of regulation in gluconeogenesis: metabolic state modulates the intracellular localization of aldolase B and its interaction with liver fructose-1,6-bisphosphatase [J]. *Biochemical Journal*. 2015;472(2):225–37.
- Arakaki TL, Pezza JA, Cronin MA, et al. Structure of human brain fructose 1,6-(bis)phosphate aldolase: Inking isozyme structure with function [J]. *Protein Sci*. 2004;13(12):3077–84.
- Endersby R, Baker SJ. PTEN signaling in brain: neuropathology and tumorigenesis [J]. *Oncogene*. 2008;27(41):5416–30.
- Shino S, Nasuno R, Takagi H. S-glutathionylation of fructose-1,6-bisphosphate aldolase confers nitrosative stress tolerance on yeast cells via a metabolic switch [J]. *Free Radical Biol Med*. 2022;193:319–29.
- Agrawal PK, Canvin DT. The pentose phosphate pathway in relation to fat synthesis in the developing castor oil seed. *Plant Physiol*. 1971May;47(5):672–5.
- Li M, He XX, Guo WX, et al. Aldolase B suppresses hepatocellular carcinogenesis by inhibiting G6PD and pentose phosphate pathways [J]. *Nature Cancer*. 2020;1(7):735–+.
- Cui GZ, Ma ZX, Liu YJ, et al. Overexpression of glucose-6-phosphate dehydrogenase enhanced the polyunsaturated fatty acid composition of *Aurantiochytrium sp.* SD116 [J]. *Algal Research-Biomass Biofuels and Bioproducts*. 2016;19:138–45.
- Zhao XM, Qiu X. Analysis of the biosynthetic process of fatty acids in *Thraustochytrium* [J]. *Biochimie*. 2018;144:108–14.
- Ren LJ, Sun GN, Ji XJ, et al. Compositional shift in lipid fractions during lipid accumulation and turnover in *Schizochytrium sp* [J]. *Bioresource Technology*. 2014;157:107–13.
- Zhang YT, Cui XW, Lin SZ, Lu T, Li H, Lu YH, Cao MF, Lin XH, Ling XP. Knockout of a PLD gene in *Schizochytrium limacinum* SR21 enhances docosahexaenoic acid accumulation by modulation of the phospholipid profile. *Biotechnol Biofuels Bioprod*. 2024Jan 30;17(1):16.
- Okuyama H, Orikasa Y, Nishida T. In vivo conversion of triacylglycerol to docosahexaenoic acid-containing phospholipids in a thraustochytrid-like microorganism, strain 12B [J]. *Biotech Lett*. 2007;29(12):1977–81.
- Ali U, Lu SP, Fadlalla T, et al. The functions of phospholipases and their hydrolysis products in plant growth, development and stress responses [J]. *Prog Lipid Res*. 2022;86:18.
- Yue XH, Chen WC, Wang ZM, Liu PY, Li XY, Lin CB, Lu SH, Huang FH, Wan X. Lipid Distribution pattern and transcriptomic insights revealed the potential mechanism of docosahexaenoic acid traffics in *Schizochytrium sp.* A-2. *J Agric Food Chem*. 2019;67(34):9683–93.
- Zhao X, Qiu X. Very long chain polyunsaturated fatty acids accumulated in triacylglycerol are channeled from phosphatidylcholine in *Thraustochytrium*. *Front Microbiol*. 2019;10:1–12.
- Anaokar S, Kodali R, Jonik B, et al. The glycerophosphocholine acyltransferase Gpc1 is part of a phosphatidylcholine (PC)-remodeling pathway that alters PC species in yeast. *J Biol Chem*. 2019Jan 25;294(4):1189–201.
- Stålberg K, Neal AC, Ronne H, Ståhl U. Identification of a novel GPCAT activity and a new pathway for phosphatidylcholine biosynthesis in *S cerevisiae*. *J Lipid Res*. 2008;49(8):1794–806.
- Lager I, Yilmaz JL, Zhou XR, et al. Plant acyl-CoA:lysophosphatidylcholine acyltransferases (LPCATs) have different specificities in their forward and reverse reactions. *J Biol Chem*. 2013Dec 27;288(52):36902–14.
- Rowlett VW, Mallampalli V, Karlstaedt A, et al. Impact of membrane phospholipid alterations in *Escherichia coli* on cellular function and bacterial stress adaptation. *Journal of Bacteriology*. 2017;199(13):e00849-16.
- Balla T. Phosphoinositides: tiny lipids with giant impact on cell regulation. *Physiol Rev*. 2013Jul;93(3):1019–137.
- Lee J, Welti R, Schapaugh WT, et al. Phospholipid and triacylglycerol profiles modified by PLD suppression in soybean seed [J]. *Plant Biotechnol J*. 2011;9(3):359–72.
- Kennedy EP, Weiss SB. The function of cytidine coenzymes in the biosynthesis of phospholipides [J]. *J Biol Chem*. 1956;222(1):193–214.
- Metz JG, Roessler P, Facciotti D, et al. Production of polyunsaturated fatty acids by polyketide synthases in both prokaryotes and eukaryotes [J]. *Science*. 2001;293(5528):290–3.

26. Jiang Z, Wang M, Nicolas M, et al. Glucose-6-Phosphate Dehydrogenases: The Hidden Players of Plant Physiology. *Int J Mol Sci.* 2022;23(24):16128.
27. Song XJ, Tan YZ, Liu YJ, et al. Different impacts of short-chain fatty acids on saturated and polyunsaturated fatty acid biosynthesis in *Aurantiochytrium sp* SD116 [J]. *Journal of Agricultural and Food Chemistry.* 2013;61(41):9876–81.
28. Liu B, Liu J, Sun PP, et al. Sesamol enhances cell growth and the biosynthesis and accumulation of docosahexaenoic acid in the microalga *Cryptocodinium cohnii* [J]. *J Agric Food Chem.* 2015;63(23):5640–5.
29. Zhang M, Fan JL, Taylor DC, et al. DGAT1 and PDAT1 acyltransferases have overlapping functions in *Arabidopsis* triacylglycerol biosynthesis and are essential for normal pollen and seed development [J]. *Plant Cell.* 2009;21(12):3885–901.
30. Zhang GY, Bahn SC, Wang GL, et al. PLDα1-knockdown soybean seeds display higher unsaturated glycerolipid contents and seed vigor in high temperature and humidity environments [J]. *Biotechnol Biofuels.* 2019;12:23.
31. Bates PD, et al. Acyl editing and headgroup exchange are the major mechanisms that direct polyunsaturated fatty acid flux into triacylglycerols. *Plant Physiol.* 2012;160(3):1530–9.
32. Liu WH, Huang ZW, Li P, et al. Formation of triacylglycerol in *Nitzschia closterium f. minutissima* under nitrogen limitation and possible physiological and biochemical mechanisms [J]. *Journal of Experimental Marine Biology and Ecology.* 2012;418:24–9.
33. Yu XJ, Sun J, Zheng JY, et al. Metabolomics analysis reveals 6-benzylaminopurine as a stimulator for improving lipid and DHA accumulation of *Aurantiochytrium sp* [J]. *J Chem Technol Biotechnol.* 2016;91(4):1199–207.
34. Liu ZX, You S, Tang BP, et al. Inositol as a new enhancer for improving lipid production and accumulation in *Schizochytrium sp* SR21 [J]. *Environ Sci Pollut Res.* 2019;26(35):35497–508.
35. Shen B, Jensen RG, Bohnert HJ. Mannitol protects against oxidation by hydroxyl radicals [J]. *Plant Physiol.* 1997;115(2):527–32.
36. Han X, Li ZH, Wen Y, et al. Overproduction of docosahexaenoic acid in *Schizochytrium sp* through genetic engineering of oxidative stress defense pathways [J]. *Biotechnology for Biofuels.* 2021;14(1):10.
37. Bass DA, Parce JW, Dechatelet LR, et al. Flow cytometric studies of oxidative product formation by neutrophils: a graded response to membrane stimulation [J]. *J Immunol.* 1983;130(4):1910–7.
38. Zorov DB, Juhaszova M, Sollott SJ. Mitochondrial reactive oxygen species (ROS) and ROS-induced ROS release. *Physiol Rev.* 2014;94(3):909–50.
39. X. J. Yu, J. Sun, Y.Q. et al. Metabolomics analysis of phytohormone gibberellin improving lipid and DHA accumulation in *Aurantiochytrium sp*. *Biochem Eng J.* 2016;112:258–68.

Publisher's Note

Springer Nature remains neutral with regard to jurisdictional claims in published maps and institutional affiliations.